JOURNAL OF SPACECRAFT AND ROCKETS
Vol. 38, No. 4, July–August 2001

Development of a Target Marker for Landing on Asteroids

Shujiro Sawai*
University of Michigan, Ann Arbor, Michigan 48109-2140
Jun'ichiro Kawaguchi†
Institute of Space and Astronautical Science, Sagamihara 229-8510, Japan
Daniel Scheeres‡
University of Michigan, Ann Arbor, Michigan 48109-2140
and
Naoki Yoshizawa§ and Masahiro Ogasawara¶
NEC Aerospace Systems, Ltd., Yokohama 224-8555, Japan

The proposed asteroid sample return mission MUSES-C calls for a spacecraft to approach an asteroid, touch down on its surface, and collect samples that will be returned to Earth. During the touchdown and sampling phase, the spacecraft will navigate relative to the asteroid surface using optical target markers placed on the asteroid surface before the final approach. By using the target marker as a reference point, navigation during the landing phase will be much more reliable and precise. Because of the microgravity environment on the asteroid surface, the settling time and dynamics of the target markers are items of interest. Thus, it is important to design the target marker with as small a coefficient of restitution as possible to minimize the settling time, which in turn minimizes the time the spacecraft must hover above the asteroid surface. To achieve this small coefficient of restitution, the target marker will be constructed out of a bag with balls stored internally. On impact, the balls will dissipate energy relative to each other and, hence, will dissipate the total energy of the target marker. To better predict the performance of such a target marker, analytical and numerical investigations are performed that model the motion of a bouncing target marker across the surface of a rotating asteroid. As a result of the analysis, some target limits on the target marker coefficient of restitution are developed. A series of microgravity tests are reported that confirm the basic design and show that the target value of coefficient of restitution can be reached.

Nomenclature

e	=	coefficient of restitution
e_b	=	coefficient of restitution of a ball in the target marker (TM) bag
e_T	=	total coefficient of restitution of a TM
g	=	local constant acceleration acting on TM
h	=	altitude of TM release
$\tilde{h}$	=	altitude of TM release normalized by mean asteroid radius
k	=	spring constant
m	=	mass of a TM plus the movable plate
m_b	=	mass of a ball in a TM
n	=	total number of balls in a TM
$\hat{\boldsymbol{n}}$	=	outward normal to asteroid surface
R_0	=	mean asteroid radius
T_i	=	time between ith and $(i+1)$th impact of TM
T_i^s	=	time between release and $(i+1)$th impact of TM
T^s	=	settling time for TM
T^{s*}	=	minimum settling time for TM, with release speed as free parameter
T_0	=	time between TM release and first impact on asteroid
U_x, U_y, U_z	=	gravitational attraction of the asteroid along the x, y, and z directions
V_i	=	TM speed normal to surface after ith rebound
V_r	=	release speed of the TM
V_r^*	=	optimal release speed of the TM, to minimize settling time
V_0	=	TM speed normal to surface at first impact
v	=	speed of the ejected TM
$\boldsymbol{v}$	=	velocity vector of TM
$\boldsymbol{v}_N$	=	velocity vector of TM normal to asteroid surface
$\boldsymbol{v}'_N$	=	velocity vector of TM normal to asteroid surface after rebound
$\boldsymbol{v}_T$	=	velocity vector of TM tangent to asteroid surface
$\boldsymbol{v}'$	=	velocity vector of TM after rebound with asteroid surface
x, y, z	=	coordinate directions along the minimum, intermediate, and maximum moment of inertia of the asteroid, respectively
x_0, x_1	=	initial and final displacement of spring
ω	=	rotation rate of the asteroid

Received 14 September 2000; revision received 6 April 2001; accepted for publication 13 April 2001.

*Visiting Scholar, Department of Aerospace Engineering; also Research Associate, Space Systems Engineering Division, Institute of Space and Astronautical Science, Sagamihara 229-8510, Japan.
†Professor, Space Systems Engineering Division.
‡Assistant Professor, Department of Aerospace Engineering.
§Staff Engineer, First System Division, First Engineering Department.
¶Manager, First System Division, First Engineering Department.

Introduction

THE Institute of Space and Astronautical Science in Japan is currently planning an asteroid sample return mission, the Mu Space Engineering Spacecraft-C mission (MUSES-C). The launch of the spacecraft is scheduled in November 2002, with a rendezvous with asteroid 1998 SF36 in October 2005. The spacecraft will stay at the asteroid for at least 2 months, during which time a number of surface samples will be obtained. Then, in December 2005 the spacecraft will begin its journey back to the Earth, arriving in June 2007. The samples will be transferred to a reentry capsule, which will be targeted to a specific site for recovery. The sample capsule will be recovered within a few days after its descent to the surface.[1]

A key part of the mission occurs when the spacecraft executes a controlled approach to the asteroid surface, touches down on the surface to retrieve a sample, and then backs away from the surface to a safe altitude.[2] During the touchdown and sampling sequence, the relative velocity between the spacecraft and the asteroid surface should be less than 10 cm/s to avoid damage to the sampling device. To control the relative motion within these constraints, a target marker (TM) will be placed on the asteroid surface before

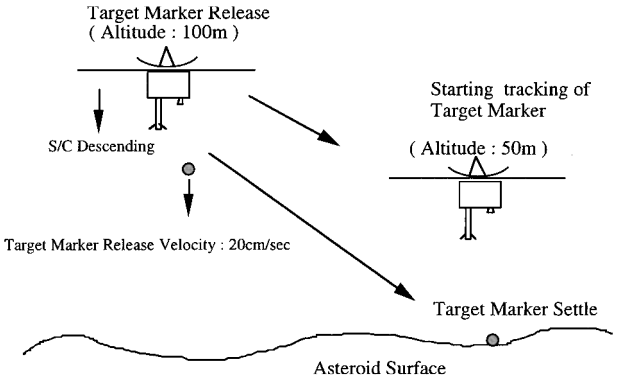

Fig. 1 Typical procedure for asteroid approach of MUSES-C mission.

the final approach and touchdown. The TM is essentially an artificial landmark on the asteroid surface and ideally has a diffuse, high reflectance relative to the background asteroid, making it is easy to detect with the onboard camera. By using the TM as a reference point, navigation will be more reliable and precise. The TM will be imaged with an onboard camera, which will use a time sequence of images to estimate the lateral motion of the spacecraft. To deploy the TM, the spacecraft will nominally initiate a descent to the surface with the proper deployment speed of the TM and release them from the bus with a small speed relative to the spacecraft. The spacecraft will then initiate a braking maneuver to maintain its altitude, while the TM will continue down to the surface. The spacecraft will also have a laser altimeter to control its descent rate and its hovering phase while the TM settle on the asteroid surface. The basic plan calls for the spacecraft to release a TM at an altitude of approximately 100 m, ideally at a speed of 20 cm/s down with no lateral speed in the asteroid fixed frame. A typical procedure for touchdown is shown in Fig. 1.

This paper will focus on the simulation and testing of the TM for the MUSES-C mission. Because of the microgravity environment on the asteroid surface (on the order of 0.01 mg), the settling time of the TM can be much longer than for a similar apparatus in a 1-g environment. Because of the design of the touchdown sequence, the spacecraft will not approach the asteroid surface until after the TM has settled on the asteroid surface. Thus, the longer the settling time is the longer the spacecraft must maintain its altitude above the asteroid surface. Because this requires a nontrivial expenditure of fuel and is an inherently unstable dynamic situation,[3] the need to reduce the settling time is clear. Thus, the main requirement for the TM (apart from having high reflectance) is that it have a low coefficient of restitution, which will minimize this settling time.

This paper primarily treats topics related to the coefficient of restitution of the TM and how this affects the settling time and dynamics of the TM. First, we discuss the basic dynamics of a bouncing body in the low-gravity environment on an asteroid surface and derive an optimal release speed for a minimum settling time. Next, a number of numerical simulations are made of this scenario to model the dynamics and response of the TM. The specific models used are discussed as appropriate, but the basic asteroid model is chosen in accordance with current best estimates of the shape, size, density, and rotation rate of the target asteroid. The use of realistic asteroid parameters and shapes will highlight some of the concerns and constraints that must be dealt with in the deployment and design of the TM, and will ensure that the analysis contains the essential qualitative features that will be encountered at the asteroid. From this discussion, we extract some necessary limits on the TM's total coefficient of restitution and gain some insight into how the deployment of the TM should occur in a real mission environment. Following this analysis, we focus on the mechanical development of the TM, which involves proposing a basic mechanism for the TM, evaluating its response using theoretical models, and performing microgravity tests on the constructed mechanism.

TM Dynamics on the Asteroid Surface

The motion of the TM from its deployment until it settles on the surface of the asteroid is investigated. When the possible motion that may occur as a function of its coefficient of restitution is understood, it is possible to derive realistic bounds on what this parameter must be. We model the interaction of the TM with the surface as an ideal bouncing ball with specified coefficient of restitution. This idealized model captures the basic effect of these interactions and can be used in conjunction with realistic models of an asteroid surface and gravity to identify the important effects that occur.

Interaction Model

We assume that the TM strikes the asteroid surface at a particular location, defined by a numerical integration of the TM's trajectory from the release condition at a given altitude above the asteroid surface. See Scheeres et al.[4] for a detailed description of current simulation techniques for trajectories in close proximity to asteroids. At the time of impact, the TM has a velocity vector $\boldsymbol{v}$ directed toward the surface of the asteroid. We assume that the asteroid surface is characterized locally as a flat, oriented plate defined by an outward normal to the surface, $\hat{\boldsymbol{n}}$. Thus, we can decompose the velocity vector into a component normal and tangent to the surface:

$$\boldsymbol{v}_N = (\hat{\boldsymbol{n}} \cdot \boldsymbol{v})\,\hat{\boldsymbol{n}} \tag{1}$$

$$\boldsymbol{v}_T = \boldsymbol{v} - (\hat{\boldsymbol{n}} \cdot \boldsymbol{v})\,\hat{\boldsymbol{n}} \tag{2}$$

Under basic assumptions of impulsive rebound,[5] the velocity tangent to the surface is unaffected, whereas the velocity component normal to the surface is reversed and diminished by the coefficient of restitution e. Thus, following impact the velocity normal to the surface is

$$\boldsymbol{v}'_N = -e\,(\hat{\boldsymbol{n}} \cdot \boldsymbol{v})\,\hat{\boldsymbol{n}} \tag{3}$$

and the new velocity becomes

$$\boldsymbol{v}' = \boldsymbol{v} - (1+e)\,(\hat{\boldsymbol{n}} \cdot \boldsymbol{v})\,\hat{\boldsymbol{n}} \tag{4}$$

To apply this model in our numerical computations, the TM's trajectory is integrated until it crosses the surface of the asteroid, yielding a sequence of two trajectory points that bracket the asteroid surface. Then a simple halving scheme for the integration step size is employed to find the actual impact point to a specified degree of accuracy. Specifically, once the surface is crossed, we halve the step size and reverse the integration direction, searching for a new crossing. Once the next crossing occurs, we continue the halving and time reversal process until the surface crossing point is isolated to within a specified degree of accuracy. The local orientation of this surface element is then found and the preceding algorithm to compute the new velocity vector $\boldsymbol{v}'$ is applied.

Mathematically, the TM will bounce an infinite number of times before dissipating all of its kinetic energy, a situation that cannot be easily computed in a numerical trajectory simulation. To deal with this, we define a certain scale height for the surface of the asteroid and assume that all rebound motion with an altitude less than this scale height will be, effectively, trapped at the current site. Thus, after every rebound, we compute the expected rebound altitude using a simplified analytical theory. If the computed altitude is less than this scale height, we terminate the integration. Although this approach is an obvious approximation, by taking the scale height to be small (on the order of centimeters), we find a reasonable model for this motion. Neglected here is the possible sliding/rolling motion of the TM over the surface. We will see later, in the test experiments, that rotational motion can be a factor in the response of the TM. Thus, our point mass interaction assumption is an approximation that should be relaxed in future studies of this problem.

For the numerical computation of the TM trajectory, we consider both motion about an ideal triaxial ellipsoid[6] and motion about an actual, measured asteroid shape.[7] For both cases, we scale the shape models to match with the currently expected size of the MUSES-C target asteroid, with a mean radius of 265 m and an assumed shape ratio of 2:1:1. Based on estimates of its spectral class, we choose a density of 3 g/cm^3. We also assume that it is in uniform rotation about its maximum moment of inertia with a rotation period of 19 h. The assumption of uniform rotation for the asteroid is valid in general, because it is well established that the majority of asteroids are in such a rotation mode due to their nonlinear stability. For the real

asteroid shape model, we take the measured shape[8] of the asteroid Castalia and uniformly scale it until its mean radius is equal to 265 m. (The original Castalia asteroid has a mean radius of about 500 m.) In this way, we introduce a realistic surface and gravity field into our analysis to simulate the effects that local topology can have on a TM as it moves over the surface. The outcomes of our simulations and analysis are dependent on the preceding assumptions, and shifts in the assumed asteroid rotation rate, shape, size, and density will lead to different quantitative results for our analysis. Nevertheless, the preceding numbers have been chosen in accord with current knowledge of likely asteroid parameters.[9] Thus, the ensuing analysis contains the essential qualitative features that will be encountered at the asteroid.

Optimal Release Conditions

As discussed earlier, it is desired to minimize the settling time of the TM on the asteroid surface. A reduction in this time allows the spacecraft to initiate its close approach sequence sooner and results in less fuel expenditure and in less time spent in an inherently dangerous situation for the spacecraft. For general purposes, we wish to derive the optimal release conditions for a suitably simplified model that will allow us to generate a single analytical formula that can be used over the entire asteroid surface.

The initial altitude at which the TM is released, h, is generally fixed. There is freedom, however, in choosing the initial release speed of the TM, V_r, by controlling the speed of the spacecraft when the TM is released. Subsequent to the TM being released, the spacecraft fires its thrusters to slow its descent, allowing the TM to continue its journey to the surface alone. When it is assumed for simplicity that there is a constant local gravitational acceleration of g (which can include rotational accelerations) and an initial velocity that only has a component normal to the surface, the first time at which the TM impacts the surface is

$$T_0 = (V_r/g)\left[\sqrt{1 + 2hg/V_r^2} - 1\right] \tag{5}$$

and its speed at first impact is

$$V_0 = \sqrt{V_r^2 + 2hg} \tag{6}$$

Following impact, the speed is reversed and equal to $V_1 = eV_0$, leading to a second impact after a time $T_1 = 2V_1/g = 2eV_0/g$. Thus, a recursive process is defined where the rebound speed after n impacts is equal to $V_n = e^n V_0$, the time between the $n-1$ and nth rebound is $T_n = 2e^n V_0/g$, and the total time from TM release to the nth rebound is

$$T_n^s = T_0 + \sum_{i=1}^{n} T_i \tag{7}$$

$$T_n^s = \frac{1}{g}[V_0 - V_r] + \frac{2V_0}{g}\frac{e(1-e^n)}{1-e} \tag{8}$$

$$T_n^s = \frac{1}{g}\sqrt{V_r^2 + 2hg}\left[1 + \frac{2e(1-e^n)}{1-e}\right] - \frac{1}{g}V_r \tag{9}$$

To complete the computation, we let $n \to \infty$ and note that $e^n \to 0$ and the total bouncing time reaches a finite limit. This yields the final settling time,

$$T^s = (1/g)\sqrt{V_r^2 + 2hg}\,[(1+e)/(1-e)] - (1/g)V_r \tag{10}$$

Then, assuming a fixed altitude, acceleration, and coefficient of restitution, we can choose the release speed to minimize the total settling time T^s by solving $\partial T^s/\partial V_r = 0$. Solving for the optimal release speed V_r^* yields

$$V_r^* = (1-e)\sqrt{hg/2e} \tag{11}$$

We see that this result makes intuitive sense because for an inelastic impact ($e \to 0$) Eq. (11) suggests a large release speed as the rebounding motion will be quickly damped, whereas for a highly elastic impactor ($e \to 1$), the equation suggests a small release speed because the initial impact speed should be minimized. The predicted settling time at this release speed is

$$T^{s*} = [2/(1-e)]\sqrt{2he/g} \tag{12}$$

For our numerical computations, we will always use a release speed approximately equal to the optimal release speed (using the total gravitational and rotational accelerations at the nominal impact site). For the actual mission, it is expected that there will be operations, attitude, and propulsion constraints that may limit the release speed, but that the release speed will be chosen to be near optimal in general.

Using nominal values of $h = 100$ m and a gravitational attraction at the surface of the asteroid of $g = 0.222$ mm/s^2, we find the optimal release speed and settling time to be

$$V_r^* = 10.5\left[(1-e)/\sqrt{e}\right] \text{ cm/s} \tag{13}$$

$$T^{s*} = 31.6\left[\sqrt{e}/(1-e)\right] \text{ min} \tag{14}$$

In Fig. 2 we show the optimal release speed and settling time as a function of coefficient of restitution for this specific case. Clearly, once a realistic asteroid gravity field is determined, the optimal conditions will vary with location over the asteroid surface. Note that this simple formula is also useful in predicting optimal release conditions over a rotating ellipsoid, where the centrifugal acceleration can be incorporated into the total surface gravity. Some specific numerical checks of this formula indicate that it is, in general, accurate to within 1 cm/s of the optimal release speed. This was found by computing settling times of numerically integrated trajectories at different release speeds. These checks were performed for a limited number of release sites using the asteroid models described earlier. The actual settling time is seen to differ from the predicted, but that is to be expected given the number of assumptions made to find this specific result.

It is also important to note how the optimal release speed and settling time vary as a function of target asteroid because it is not unusual for an asteroid mission to choose an alternate target late in the development phase. In these formulas, the effect of switching asteroids is governed by the surface acceleration g, which is proportional to the asteroid density and radius R_0. Thus, the optimal release speed will be proportional to $\sqrt{(hR_0)}$, and the settling time will be proportional to $\sqrt{(h/R_0)}$. To keep the settling time constant between asteroids implies that we choose the normalized altitude to be a constant, $h/R_0 \sim \tilde{h}$. Thus, the optimal release speed for a fixed settling time will vary linearly with the mean asteroid radius.

Effect of Ellipsoidal Shape and Rotation

We first examine the effect of coefficient of restitution on TM surface trajectories over a uniformly rotating ellipsoid. The basic equations of motion and gravitational potential description may be found in Ref. 6. We choose the shape, size, density, and rotation period of the asteroid according to the current plausible parameters that fit observations. Of particular interest is the ensemble of possible trajectories that a TM may have, given some uncertainty in its initial position and release speed. To model this effect, we performed a series of Monte Carlo (MC) runs centered around a few specifically chosen release conditions. For each MC run we chose an initial position error of 10 m and an initial velocity error of 1 cm/s. These numbers are smaller than the true uncertainties that are expected, and, thus, the TM dispersions that we find may be smaller than occur in mission operations. In this sense, these runs provide an indication of the sensitivity of the TM dynamics as a function of release location.

The relevant equations of motion, expressed in the asteroid-fixed frame centered at its center of mass and with coordinates x-y-z taken along the axis of minimum, intermediate, and maximum moment of inertia, respectively, can be given as

$$\ddot{x} = 2\omega\dot{y} + \omega^2 x + U_x \tag{15}$$

$$\ddot{y} = -2\omega\dot{x} + \omega^2 y + U_y \tag{16}$$

$$\ddot{z} = U_z \tag{17}$$

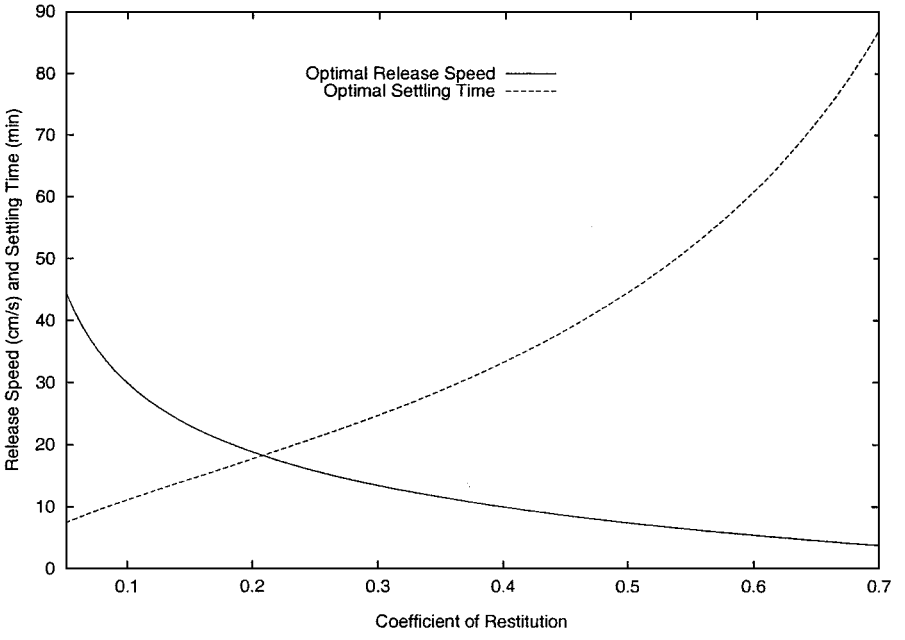

Fig. 2 Optimal release speed and settling time for a TM released 100 m over the surface of our model asteroid.

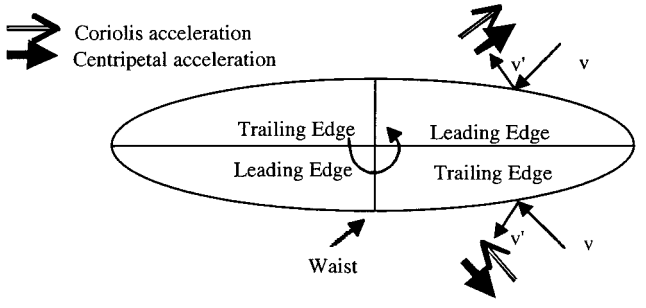

Fig. 3 TM deviations at leading edge and trailing edge; asteroid rotation pole is out of the plane of the paper.

where we assume the uniform rotation rate to be ω and its spin axis to be aligned with the z axis. U_x, U_y, and U_z are the gravitational attraction along the x, y, and z directions, respectively.

If we assume an ellipsoid for the gravity distribution and body surface, then there will be a trend for the impacting TM to have its recoil velocity move in the direction of greatest slope. On an ellipsoid, this tendency will cause a bouncing body to move away from the ends of the body and toward the narrow waist that contains the y–z plane. This tendency, due to the shape of the body, must be balanced against the effect of Coriolis and centrifugal accelerations that act on the body. The Coriolis acceleration will tend to rotate the velocity vector of the body in a clockwise direction (relative to the rotation pole), whereas the centrifugal acceleration will tend to pull the body away from the asteroid, generally acting in the opposite direction of gravity. For a slowly rotating asteroid, these effects are negligible. However, even for a 19-h rotation period, these body rotation effects can be clearly discerned. In general, these rotation effects lead to an asymmetry between an impact on the leading edge and trailing edge of the body. After impact on a leading edge, the resulting velocity vector of the body will be pulled away from the surface, with the centrifugal and Coriolis accelerations pulling in the same direction, which tends to lengthen the flight time between impacts and allows leading-edge impactors to move over greater distances on the body. Conversely, for a trailing-edge impactor, the Coriolis and centrifugal accelerations tend to fight each other, resulting in a shorter flight time and less dispersion (see Fig. 3)

These effects are clearly seen in Fig. 4, where a leading-edge impact distribution (longitude between 0 and 90 deg) has a clear downstream motion, whereas the trailing-edge impact distribution (longitude between −90 and 0 deg) tends to be more tightly compacted. In Fig. 4a, these effects are clearly evident for a large coefficient of restitution ($e = 0.5$) , although in Fig. 4b the effect is still visible for a smaller coefficient value ($e = 0.1$).

A few additional runs were also performed with an increased asteroid rotation rate. In these runs we saw this asymmetry become more pronounced, with the leading-edge distribution becoming more spread out, whereas the trailing-edge distribution retained its close packing.

Effect of Irregular Shape

Also affecting the dynamics of the impacting TMs will be the local topology of the asteroid. Because of the (likely) nonsmooth surface of the body, the statistics of the impacting TMs will be further modified. Over some regions, the local topology can serve to focus the trajectories, causing the distribution to become more tightly packed, whereas in other regions, the topology can force a strong separation in the distribution. These areas are naturally identified with the local shape of the asteroid, convex regions being more likely to trap the TM and concave regions being more likely to disperse the trajectories. We show two MC runs in Fig. 5. The coefficient of restitution for these runs was set at a small value of 0.1. Both of the impact sites are in the same general surface area of the asteroid, but one occurs in a region where there is a stronger topology variation, characterized by a ridge running through the nominal impact site, which causes the rebounding TMs to become more widely dispersed. Such local effects cannot be effectively characterized until the actual asteroid surface topology is known, and the potential landing sites chosen. Qualitative study is still possible, however, using existing models of asteroid surfaces.

Constraints on TM Design and Release Conditions

A number of basic constraints on the TM design and release conditions can be formulated, given the preceding discussion. We see that considerations from settling time and surface dispersions all push us to reduce the coefficient of restitution to as small a value as possible. Because the surface dispersion requirements are not clearly formulated yet for the mission, the natural constraint will arise from the settling time. Choosing a target value of $e \sim 0.1$ yields a theoretical settling time of 10 min, which is a reasonable time span for the settling to occur. A series of MC runs at various sites over the ellipsoid asteroid model with the same basic release conditions and coefficient of restitution show that the actual settling times will be on the order of 10 min or less, with some notable exceptions. In Fig. 6 we show a total of 5000 MC simulations of

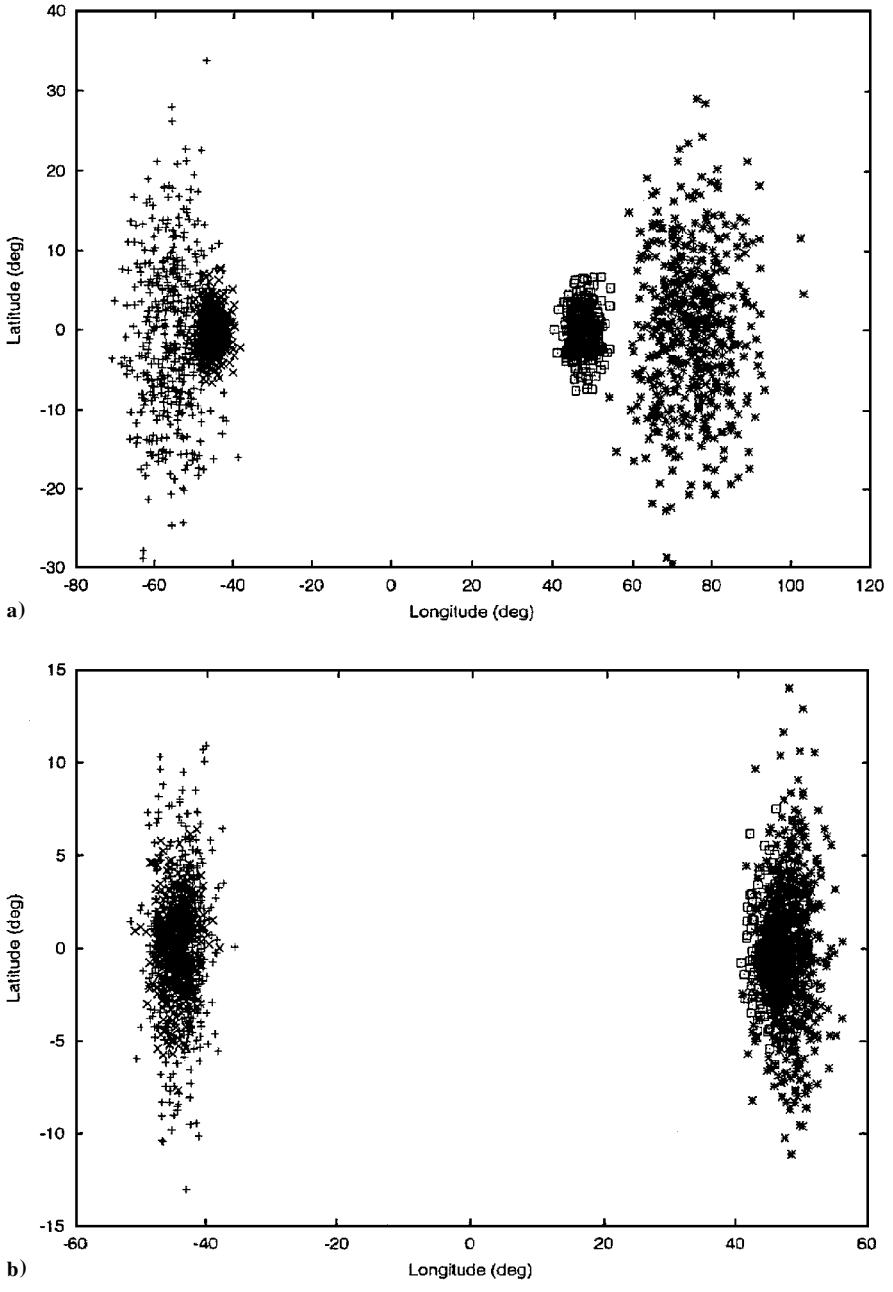

Fig. 4 Latitude vs longitude plots of MC simulations of TM impacts with an ellipsoid surface: tightly gathered points (□ and ×) indicate location of first impact on the surface, dispersed points (+ and *) indicate final location on the surface once the TMs have settled: a) coefficient of restitution for this run set at large value of 0.5 and b) coefficient of restitution for this run set at value of 0.1.

impact on the ellipsoid asteroid surface, starting from an altitude of 100 m with an optimal release speed chosen according to our simple analysis and with a specified coefficient of restitution of 0.1. Figure 6 shows distance from the initial impact point vs total settling time, thus indicating how far the TM travels, as well as how long it takes for it to settle on the surface. The series of cases with long settling times are all for nominal impact sites near the long end of the ellipsoid, indicating that this may be a poor area for a sampling site. Overall, however, this indicates that a target value of 0.1 will work.

Another item that comes out of these analyses is that the dispersion statistics of the TM will be affected by the location chosen on the asteroid surface. Whereas the effects of dispersion tend to be minimized for a coefficient of restitution set at 0.1, it is still clear that local topology can play a strong role in controlling how the TMs are distributed. Such concerns cannot be realistically addressed, however, until the actual asteroid shape and gravity are estimated after rendezvous, and the desired landing locations located. By this time, the TM design will be fixed, of course, meaning that certain locations on the asteroid may be deemed unacceptable for TM deployment, due to local topography conditions. The determination of whether a location will be problematic will most likely be done by performing series of MC simulations of landings at that site.

Proposed Mechanism for the TM

To meet the requirements of the previous studies a basic TM design has been proposed, consisting of a bag covered with reflective material and filled with a number of balls with some value of coefficient of restitution. With this simple design, the basic requirements for the TM can be achieved. When the TM hits the asteroid surface, the balls inside the bag will collide with each other and dissipate the total energy of the bag system. Depending on the design of the bag and the shapes, numbers, and coefficients of restitution of the balls, the total coefficient of restitution of the entire system will vary.

There are many different parameters for possible optimization in this design, including the shape of the bag, material and thickness of the bag, shape and material properties of the balls, and others.

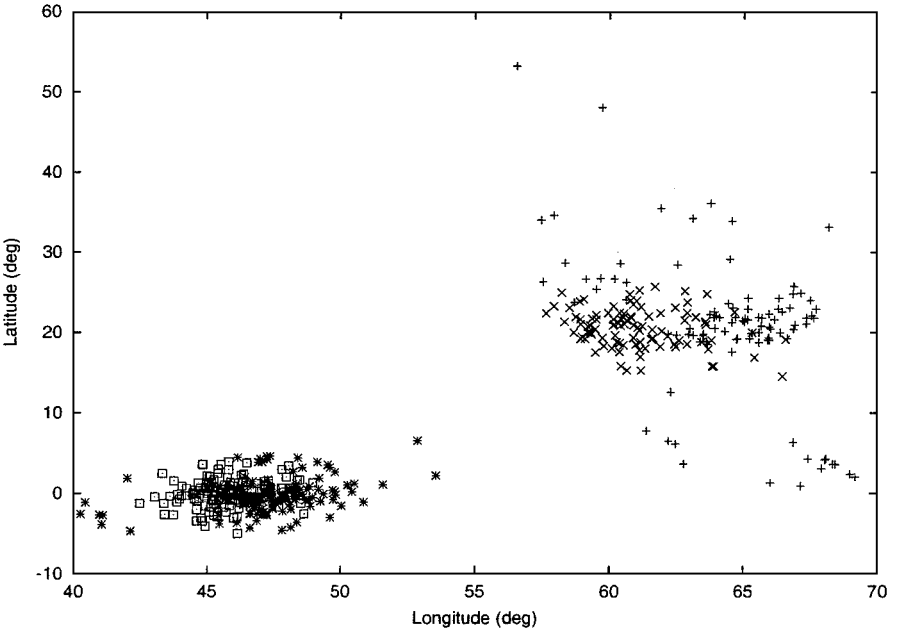

Fig. 5 Latitude vs longitude plots of MC simulations of TM impacts with a realistic asteroid surface: tightly gathered points (□ and ×) indicate location of first impact on the surface, dispersed points (+ and *) indicate the final location on the surface once the TMs have settled.

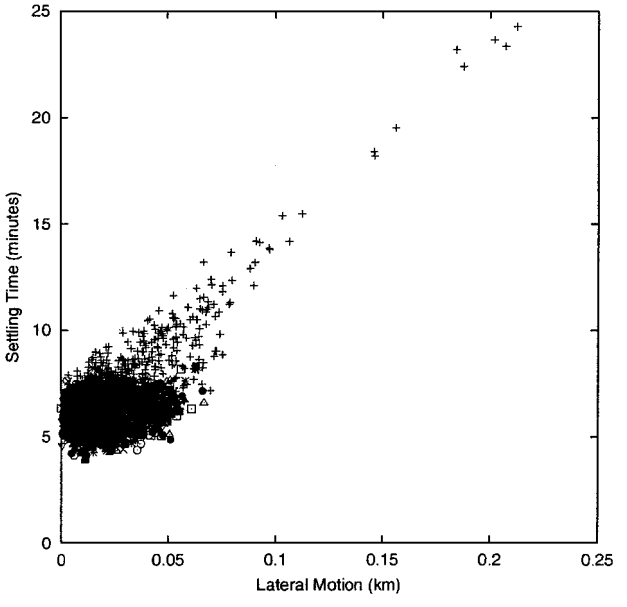

Fig. 6 Scatter plot of settling time vs lateral motion for a series of impact simulations on the surface of the nominal ellipsoid asteroid model.

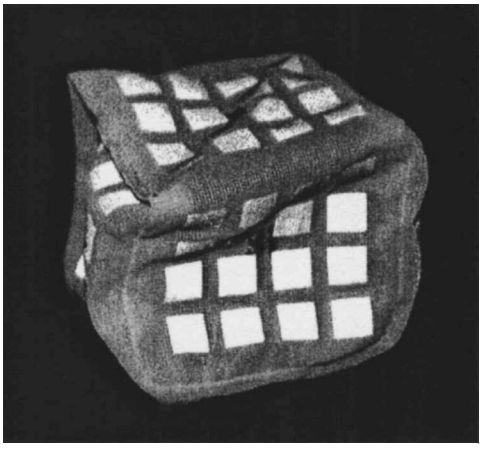

Fig. 7 Photograph of TM (prototype).

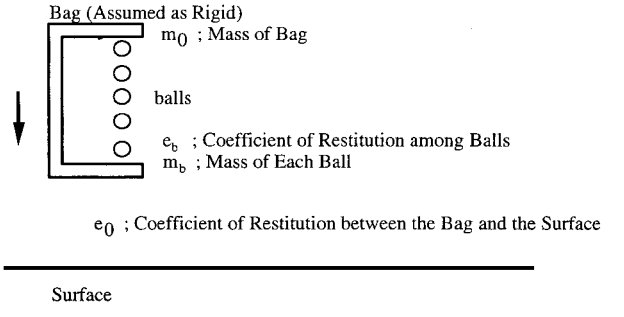

Fig. 8 Configuration of simplified one-degree-of-freedom simulation.

To simplify the design and testing process, however, a number of constraints were enforced. Namely, the properties of the bag were fixed, and the balls were assumed to be of uniform shape and material. Thus, the optimization of the TM coefficient of restitution will then just be a function of the number of balls and their size. Figure 7 shows the basic proposed design for the system.

Simple Simulation of TM Bounce

To give an initial evaluation of the described concept, some simple numerical simulations of a bouncing TM were conducted. Figure 8 shows the assumed configuration for the simulation. Motion was restricted to have one degree of freedom, and the bag was assumed to form a rigid boundary (for analytical tractability). The dynamics of motion are similar to those developed earlier to model the simple impact dynamics of the TM. Figure 9 shows an example of the motion of the balls inside a bag as the TM bounces.

The simulated relation between the coefficient of restitution of the balls and the overall coefficient of restitution of the TM is summarized in Fig. 10. Figure 10 suggests that, even if the coefficient of restitution among the balls is relatively large, the overall coefficient of restitution can be small. Figure 11 shows the influence of the number of balls inside the bag. From these simulations we can infer that

$$e_T \sim e_b^n \tag{18}$$

Thus, these simple simulations indicate that increasing the number of balls in the bag will generally decrease the total coefficient of restitution and that the relative coefficient of restitution among the balls is not an important parameter. Figure 12 shows the influence of the coefficient of restitution between the bag and the asteroid surface.

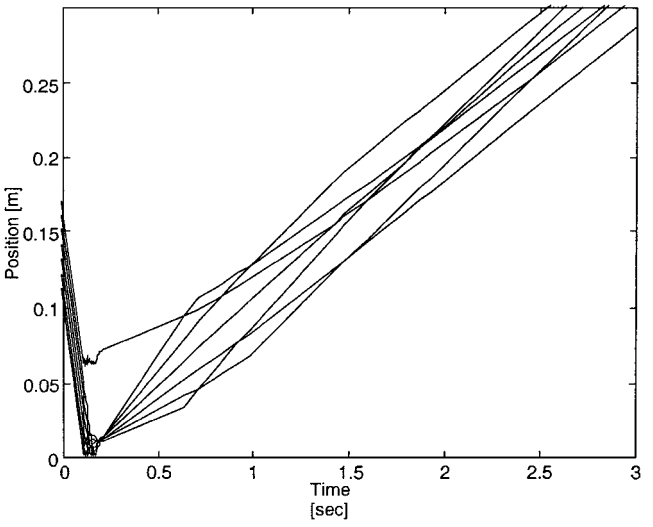

Fig. 9 Example of motion of balls (number of balls is 5 and coefficient of restitution is 0.7 this simulation).

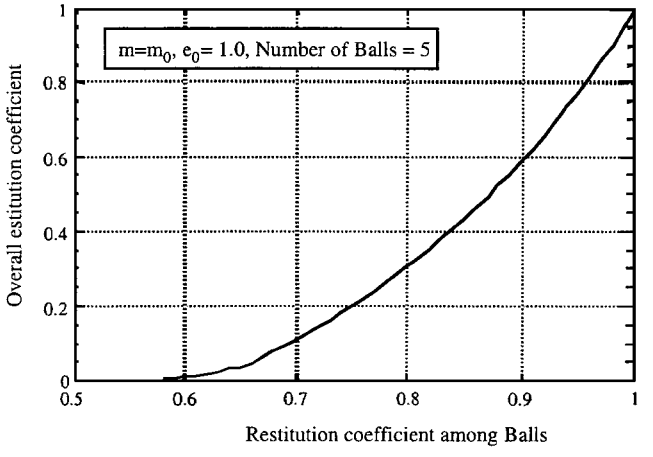

Fig. 10 TM overall coefficient of restitution vs coefficient among balls.

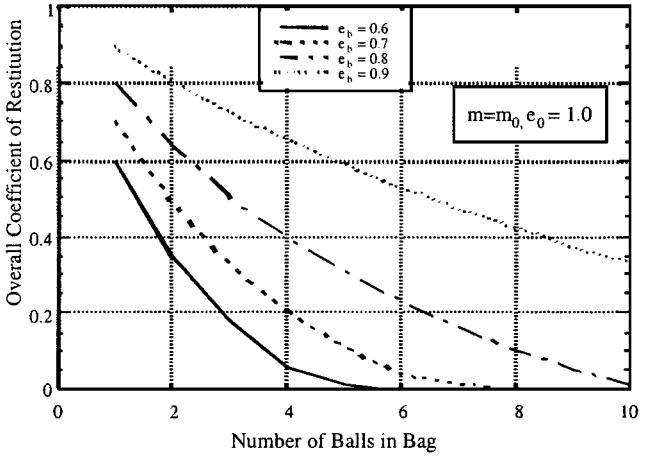

Fig. 11 TM overall coefficient of restitution vs number of balls.

Hardware Tests in a Microgravity Environment

To evaluate the coefficient of restitution of a prototype TM, a series of microgravity tests were conducted at the drop-shaft microgravity experiment system at the Japan Microgravity Center. The length of the drop shaft is over 700 m, and it has an ability to provide a microgravity environment for approximately 10 s. This was a sufficient time for one rebound of the TM to occur and its coefficient of restitution to be measured. Seven types of TMs were tested, as listed in Table 1.

Table 1 TM tested at microgravity tests

TM contents	Mass of contents, g	Impact velocity, cm/s
Spherical balls, 2-mm diam	50, 100, 300	30
Spherical balls, 6-mm diam	50, 100, 300	30
Empty bag	N/A	30

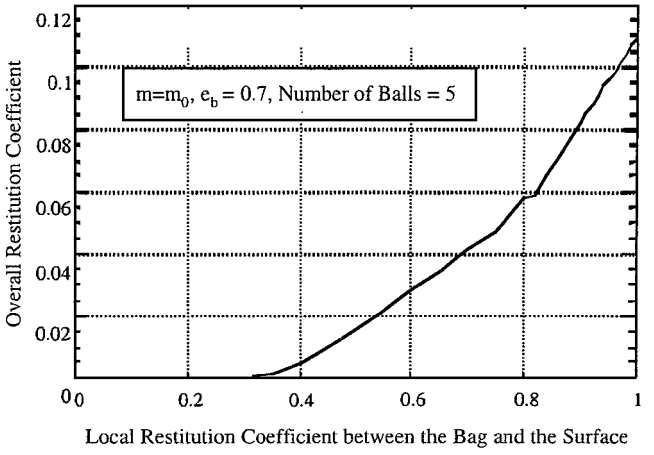

Fig. 12 TM overall coefficient of restitution vs coefficient of bag.

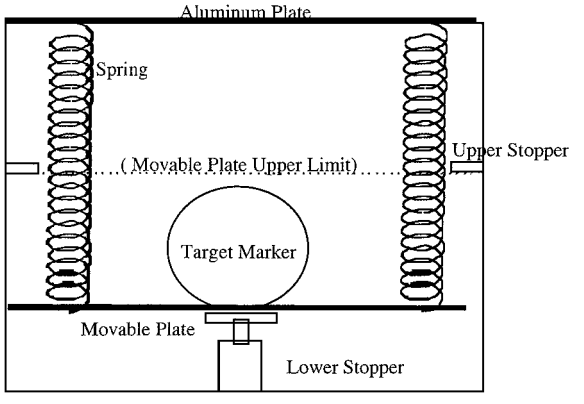

Fig. 13 TM eject apparatus for microgravity tests.

For each test, as soon as the microgravity environment was achieved, the TMs were accelerated with springs to a preset velocity and then hit an aluminum plate after a few seconds of travel. The motions of the TMs were recorded with video camera to trace their trajectories.

The apparatus that lets the TMs hit the plate with constant velocity has a simple mechanism, as shown in Fig. 13. It consists of a movable plate, a spring with spring coefficient k (N/m), and two stoppers. The TMs are set on the movable plate. Initially the apparatus is in a 1-g environment, and the spring is pushed down to the lower stopper with a spring elongation of x_1. Once the microgravity environment is achieved, the spring is released and pushes the plate to the upper stopper at a distance x_0. By neglecting drag and transverse forces during the deployment from 1 to 0 g, energy conservation holds:

$$\tfrac{1}{2}mv^2 + \tfrac{1}{2}kx_0^2 = +\tfrac{1}{2}kx_1^2 \tag{19}$$

and leads to an ejected velocity of

$$v = \sqrt{(k/m)\left(x_1^2 - x_0^2\right)} \tag{20}$$

where m is the combined mass of the movable plate and the TM.

The typical motion of a TM is shown in Fig. 14. Origins of time and position are taken with respect to the video camera coordinate, and so only the relative motion shown in Fig. 14 is of interest. In this case, the TM approached the surface with a speed of approximately 30 cm/s and rebounded from it at a speed of approximately 0.5 cm/s. The coefficient of restitution can be estimated from the gradients of the entry trajectory and the reflection trajectory.

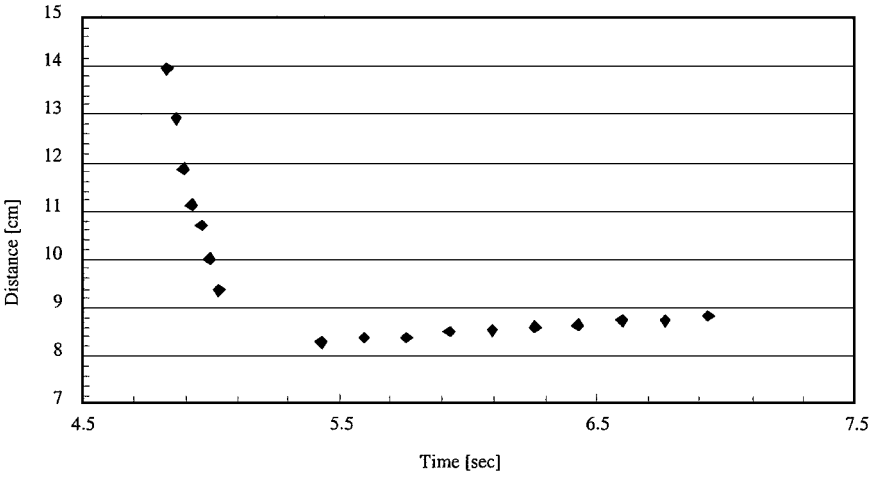

Fig. 14 Typical trajectory of the TM at microgravity environment.

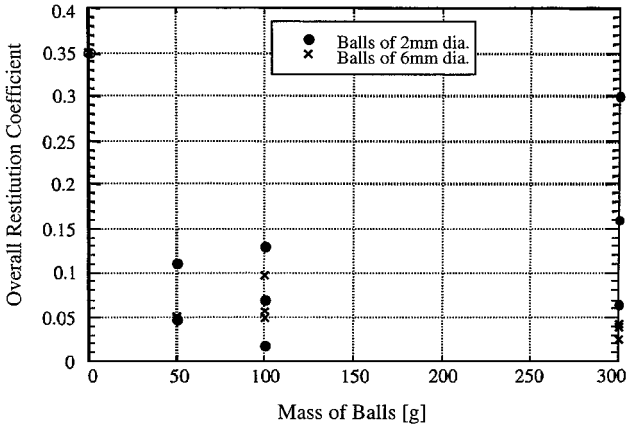

Fig. 15 Overall coefficient of restitution under microgravity environment.

The results of the experiments are summarized in Fig. 15. From the tests, we infer that there is an optimal number of balls to place within the bag. If the bag is filled with an excessive number of balls, then the balls cannot move freely relative to each other, which results in a decrease in the number of local collisions and an increase in the total coefficient of restitution. The data shown in Fig. 15 also indicate that the coefficient of restitution can differ from experiment to experiment, even if all of the parameters of the TM are held constant. This variation is probably due to the transfer of translational kinetic energy to rotational kinetic energy of the TM. If such a transfer occurs, the effective coefficient of restitution of the TM will appear smaller for that bounce. Actually, some of the translational kinetic energy has been stored in the rotational kinetic energy of the TM and may be converted back into translational kinetic energy at a later impact, which would result in a larger coefficient of restitution for the later bounce. This explains the observed small value of coefficient of restitution in Fig. 15. To better understand these situations will involve the simulation of rigid-body interactions with an asteroid surface and are items for future study.

Conclusions

An analysis of the design and dynamics of TMs for use on the surface of an asteroid was made. Such TMs will be used by the MUSES-C mission to aid in their sampling experiment at the target asteroid 1998 SF36. A target value of coefficient of restitution of the TMs was chosen based on an analysis of TM dynamics on the surface of the asteroid. Then a proposed solution and its verification were presented. The solution assumed that the TM is constructed out of a bag filled with balls. It is shown that, with such a TM design, it is possible to achieve target values for coefficient of restitution of 0.1. Some areas of future study are also identified, most importantly, the combined rotational and translational dynamics of a TM bouncing on an asteroid surface. Similar simulation methods to the ones presented here may be used to characterize specific landing sites once the MUSES-C spacecraft arrives at its target asteroid.

Acknowledgments

Support for S. Sawai for his stay at the University of Michigan as a visiting scholar was from a Fellowship from the Ministry of Education, Japan. Some of the experimental analysis described here was carried out as a part of "Ground Research Announcement for Space Utilization" promoted by Japan Space Forum. The authors would like to thank K. Ninomiya of NEC Aerospace Systems, Ltd., for his support in the analysis of the experimental results. This paper was presented as Paper AAS 00-171 at the 2000 Spaceflight Mechanics Meeting, Clearwater, Florida.

References

[1]Kawaguchi, J., "MUSES-C, Asteroid Sample and Return Journey and Its Technology Development," 49th International Astronautical Congress, IAA Rept. 11.2.5, Sept. 1998.

[2]Hashimoto, T., Kubota, T., Kawaguchi, J., Uo, M., Baba, K., and Yamashita, T., "Autonomous Descent and Touch-Down via Optical Sensors," American Astronautical Society, 11th Space Flight Mechanics Meeting, AAS Paper 01-134, Feb. 2001.

[3]Scheeres, D. J., "Stability of Hovering Orbits Around Small Bodies," American Astronautical Society/AIAA Spaceflight Mechanics Meeting, AAS Paper 99-159, Feb. 1999.

[4]Scheeres, D. J., Williams, B. G., and Miller, J. K., "Evaluation of the Dynamic Environment of an Asteroid: Applications to 433 Eros," *Journal of Guidance, Control, and Dynamics*, Vol. 23, No. 3, 2000, pp. 466–475.

[5]Greenwood, D. T., *Principles of Dynamics,* 1st ed., Prentice–Hall, Upper Saddle River, NJ, 1965, pp. 152–156.

[6]Scheeres, D. J., "Dynamics About Uniformly Rotating Tri-Axial Ellipsoids—Applications to Asteroids," *Icarus*, Vol. 110, No. 2, 1994, pp. 225–238.

[7]Scheeres, D. J., Ostro, S. J., Hudson, R. S., and Werner, R. A., "Orbits Close to Asteroid 4769 Castalia," *Icarus*, Vol. 121, No. 1, 1996, pp. 67–87.

[8]Hudson, R. S., and Ostro, S. J., "Shape of Asteroid 4769 Castalia (1989 PB) From Inversion of Radar Images," *Science*, Vol. 263, No. 5149, 1994, pp. 940–943.

[9]Scheeres, D. J., "Trajectories in Close Proximity to Asteroids," Near Earth Asteroid Sample Return Workshop, Lunar and Planetary Inst., LPI Abstract 8009, Houston, TX, Dec. 2000.

D. B. Spencer
Associate Editor